LETTER

Barrier crossing in the presence of multi-exponential memory functions with unequal friction amplitudes and memory times

A Letters Journal Exploring the Frontiers of Physics

August 2020

EPL, **131** (2020) 40004
doi: 10.1209/0295-5075/131/40004

www.epljournal.org

Barrier crossing in the presence of multi-exponential memory functions with unequal friction amplitudes and memory times

Laura Lavacchi[1], Julian Kappler[2] and Roland R. Netz[1]

[1] *Freie Universität Berlin, Fachbereich Physik - 14195 Berlin, Germany*
[2] *University of Cambridge, Department of Applied Mathematics and Theoretical Physics - Cambridge, UK*

received 18 May 2020; accepted in final form 4 August 2020
published online 7 September 2020

PACS 05.10.Gg – Stochastic analysis methods (Fokker-Planck, Langevin, etc.)

Abstract – We study the non-Markovian Langevin dynamics of a massive particle in a one-dimensional double-well potential in the presence of multi-exponential memory by simulations. We consider memory functions as the sum of two or three exponentials with different friction amplitudes γ_i and different memory times τ_i and confirm the validity of a previously suggested heuristic formula for the mean first-passage time τ_{MFP}. Based on the heuristic formula, we derive a general scaling diagram that features a Markovian regime for short memory times, an asymptotic long-memory-time regime where barrier crossing is slowed down and τ_{MFP} grows quadratically with the memory time, and a non-Markovian intermediate regime where barrier crossing is slightly accelerated or slightly slowed down, depending primarily on the particle mass. The relative weight of different exponential memory contributions is described by the scaling variable γ_i/τ_i^2, *i.e.*, memory contributions with long memory times or small amplitudes are negligible compared to other memory contributions.

Introduction. – Most rare events in biology and chemistry at the nano-scale, *e.g.*, chemical reactions and protein folding, are governed by thermal noise and can be described by Langevin or Fokker-Planck equations. Often these processes are approximated by barrier-crossing events in a one-dimensional reaction-coordinate landscape [1–10]. The Markovian approximation assumes that all orthogonal degrees of freedom relax faster than the diffusive and inertial time scales of the reaction coordinate [11–16]. However, this approximation is not always valid, for example for dihedral barrier dynamics in peptides and ion-pairing kinetics, the characteristic time scales of the reaction coordinate and the environment are similar and, therefore, one has to account for non-Markovian effects [17–23]. It was shown that for single-exponential memory, for long memory time the mean first-passage time (MFPT) τ_{MFP} follows an asymptotic power law $\tau_{MFP} \simeq \tau^2/\gamma$ as a function of the memory time τ and the friction coefficient γ [24]. This means that in the presence of very slowly decaying memory, the barrier-crossing kinetics is modified even when the MFPT is much longer than the memory time; thus, simple time-scale separation, according to which memory should only influence the MFPT up to time scales of the memory time itself, breaks down. For intermediate values of the memory time and in the friction-dominated regime, memory was shown to speed up barrier-crossing kinetics, meaning that the MFPT becomes shorter than in the Markovian limit [24]. Thus, whether memory speeds up or slows down reaction kinetics depends on the precise value of the memory time. For most systems, memory effects are not characterized by one time scale and one necessarily has to take into account several memory time scales depending on the complexity of the system [11,17,25–28]. Very recently it was shown that for bi-exponential memory and the restricted case where both exponentials contribute equally to the total friction, the barrier-crossing time becomes independent of the longer memory time if at least one of the two memory times is larger than the intrinsic diffusion time [29]. In the present work, we focus on barrier crossing in the presence of a memory function that is written as a sum of two or three exponentials with unequal friction amplitudes and we confirm that a previously proposed heuristic formula for the mean first-passage time τ_{MFP} [29] is valid also when the friction amplitudes and memory times of the individual exponential memory contributions vary widely. Based on the heuristic formula, we show that the weights of individual exponential memory contributions are governed by the scaling variables γ_i/τ_i^2, meaning that memory contributions with long memory times or

small friction amplitudes become negligible compared to other memory contributions. We construct a general scaling diagram for bi-exponential memory in terms of the scaling variables γ_1/τ_1^2 and γ_2/τ_2^2 that displays a Markovian regime for large γ_1/τ_1^2 and γ_2/τ_2^2, an asymptotic non-Markovian regime for small γ_1/τ_1^2 and γ_2/τ_2^2 where τ_{MFP} grows quadratically with the memory times, and non-Markovian intermediate regimes where barrier crossing is slightly accelerated or slightly slowed down, depending on particle mass and the friction amplitude ratio γ_1/γ_2.

To proceed, we consider the generalized Langevin equation (GLE) [10,30–35]

$$m\ddot{x}(t) = -\int_0^t \Gamma(t-t')\dot{x}(t')\mathrm{d}t' - U'(x(t)) + F_R(t), \quad (1)$$

where m is the effective mass of the reaction coordinate x, $\Gamma(t)$ is the memory kernel function and $U'(x)$ is the derivative of the potential $U(x)$. $F_R(t)$ denotes the Gaussian time-dependent random force with $\langle F_R(t)\rangle = 0$. In equilibrium, which is the scenario we consider in this paper, the relation between the friction kernel $\Gamma(t)$ and the autocorrelation of the random force is

$$\langle F_R(t)F_R(t')\rangle = k_BT\Gamma(|t-t'|), \quad (2)$$

where T is the temperature and k_B is the Boltzmann constant. In non-equilibrium situations, this relation is not satisfied anymore and one has to deal with in general two distinct functions, namely the memory function and the noise correlation function [21,36]. In fact, non-equilibrium scenarios with colored noise have been shown to be useful for accelerating simulations [37].

We choose a symmetric double-well potential

$$U(x) = U_0\left[\left(\frac{x}{L}\right)^2 - 1\right]^2, \quad (3)$$

where the separation between the two wells is $2L$ and the barrier height is defined by U_0. In the main part of this article we use $U_0 = 3k_BT$.

We consider the memory kernel as a sum of N exponentials

$$\Gamma(t) = \sum_{i=1}^{N} \frac{\gamma_i}{\tau_i} e^{-t/\tau_i}, \quad (4)$$

where τ_i and γ_i are the memory times and friction coefficients. Accordingly, the random force in eq. (1) can be decomposed as

$$F_R(t) = \sum_{i=1}^{N} f_{R_i}(t), \quad (5)$$

where

$$\langle f_{R_i}(t) f_{R_j}(t')\rangle = k_BT\frac{\gamma_i}{\tau_i} e^{-|t-t'|/\tau_i}\delta_{ij}. \quad (6)$$

The integral over the memory function $\gamma = \int_0^\infty \Gamma(t)\mathrm{d}t = \sum_{i=1}^N \gamma_i$ defines the total friction coefficient and by construction is independent of the memory times. For ease of discussion, we introduce two effective time scales,

$$\tau_D = \frac{L^2\gamma}{k_BT}, \quad (7)$$

$$\tau_m = \frac{m}{\gamma}. \quad (8)$$

The diffusion time τ_D is the time it would take the particle in the overdamped limit and in the absence of a potential to diffuse by L, the inertial time τ_m characterizes the time scale of viscous dissipation of particle momentum. For $N = 2$ we can thus describe the system by $U_0/(k_BT)$ and three dimensionless time-scale ratios $\tau_m/\tau_D, \tau_1/\tau_D$ and τ_2/τ_D. To simulate the GLE in an efficient manner, we couple auxiliary variables with relaxation times τ_i and friction coefficients γ_i to the particle, as explained in the appendix [38]. The numerical simulations are based on a fourth-order Runge-Kutta integration scheme [39,40]. From the simulations, we obtain the first-passage time (FPT) distribution, defined as the distribution of times necessary for the particle to go from one potential minimum to the other for the first time. By averaging over the FPT distribution we obtain the mean first-passage time (MFPT) τ_{MFP}.

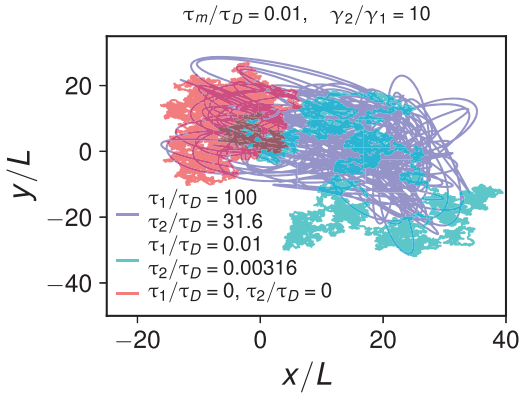

Fig. 1: Two-dimensional particle trajectories for $\tau_m/\tau_D = 0.01$ and $\gamma_2/\gamma_1 = 10$ without an external potential for the Markovian case $\tau_1/\tau_D = \tau_2/\tau_D = 0$ (red), for bi-exponential memory with $\tau_1/\tau_D = 0.01, \tau_2/\tau_D = 0.00316$ (green) and $\tau_1/\tau_D = 100, \tau_2/\tau_D = 31.6$ (blue).

To illustrate the effects of memory on the dynamics we plot in fig. 1 particle trajectories in two spatial dimensions for vanishing potential $U(x, y) = 0$ and for various memory times τ_1/τ_D and τ_2/τ_D for $\tau_m/\tau_D = 0.01$ and $\gamma_2/\gamma_1 = 10$. One clearly sees drastic differences between the Markovian case (red) for $\tau_1/\tau_D = \tau_2/\tau_D = 0$, the intermediate-memory case (green) for $\tau_1/\tau_D = 0.01, \tau_2/\tau_D = 0.00316$ and the long-memory case (blue) for $\tau_1/\tau_D = 100, \tau_2/\tau_D = 31.6$, the longer the memory times are, the more persistent the particle trajectories become.

Results. – We first consider bi-exponential memory. Figure 2(a) shows the rescaled MFPT τ_{MFP}/τ_D as a function of τ_1/τ_D for fixed $\tau_m/\tau_D = 1$ and $\gamma_2/\gamma_1 = 2$. Different colors in fig. 2(a) label different values of τ_2/τ_D.

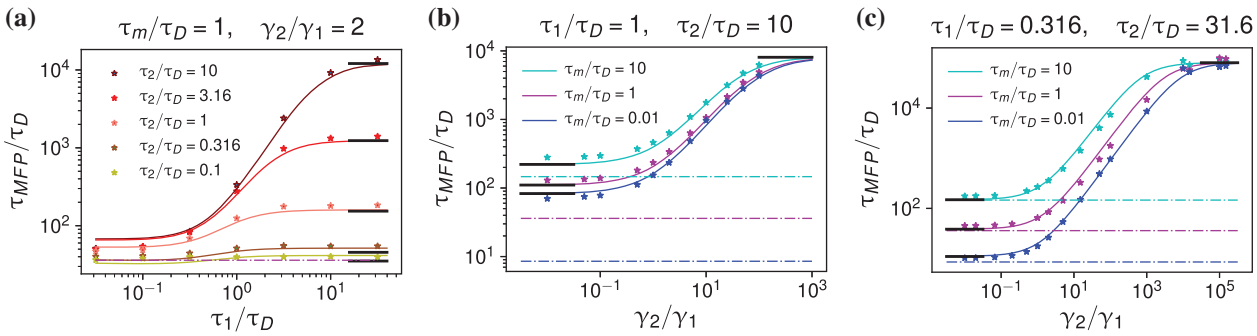

Fig. 2: Mean first-passage time for bi-exponential memory and $U_0/k_BT = 3$: (a) the rescaled MFPT τ_{MFP}/τ_D as a function of τ_1/τ_D for several values of τ_2/τ_D and fixed $\tau_m/\tau_D = 1$, $\gamma_2/\gamma_1 = 2$. (b) τ_{MFP}/τ_D for fixed $\tau_1/\tau_D = 1$, $\tau_2/\tau_D = 10$ as a function of γ_2/γ_1 for several values of τ_m/τ_D, (c) τ_{MFP}/τ_D for fixed $\tau_1/\tau_D = 0.316$, $\tau_2/\tau_D = 31.6$ as a function of γ_2/γ_1 for several values of τ_m/τ_D. Stars show the simulation results and colored lines represent the heuristic formula (9). The horizontal dash-dotted lines represent the Markovian limit, corresponding to $\tau_1 = \tau_2 = 0$. In plot (a) the black horizontal lines for high τ_1/τ_D values denote the single-exponential limit, *i.e.*, $\gamma_1 = 0$. The horizontal black lines in (b) and (c) denote the single-exponential memory kernel limit for $\gamma_2 = 0$ on the left and $\gamma_1 = 0$ on the right, in the latter limit the three black lines lie on top of each other.

We observe that in the right part of the plot, *i.e.*, for $\tau_2/\tau_D \ll \tau_1/\tau_D$, the value of the MFPT becomes independent of τ_1/τ_D, *i.e.*, the value of the longer memory time becomes irrelevant.

We compare our results for the MFPT with a heuristic crossover formula that was previously proposed based on simulations for bi-exponential memory functions, $N = 2$, with equal amplitudes γ_1 and γ_2 [29]

$$\tau_{MFP} = \sum_{i=1}^{N} \tau_{OD}^i + \left(\sum_{i=1}^{N} 1/\tau_{ED}^i \right)^{-1}, \tag{9}$$

which is the sum of the overdamped contribution

$$\frac{\tau_{OD}^i}{\tau_D} = \frac{\gamma_i e^{\beta U_0}}{\gamma \beta U_0} \left[\frac{\pi}{2\sqrt{2}} \frac{1}{1 + 10\beta U_0 \tau_i/\tau_D} + \sqrt{\beta U_0 \frac{\tau_m}{\tau_D}} \right] \tag{10}$$

and the energy-diffusion contribution to the MFPT

$$\frac{\tau_{ED}^i}{\tau_D} = \frac{\gamma e^{\beta U_0}}{\gamma_i \beta U_0} \left[\frac{\tau_m}{\tau_D} + 4\beta U_0 \left(\frac{\tau_i}{\tau_D} \right)^2 + \sqrt{\beta U_0 \frac{\tau_m}{\tau_D}} \right], \tag{11}$$

where $\beta^{-1} = k_BT$.

The heuristic formula (9) is shown by continuous lines in fig. 2(a) and is seen to describe the numerical data very accurately. The black horizontal lines to the right denote the predictions of the heuristic formula in the single-exponential case and are obtained by setting $\gamma_1 = 0$ in eq. (9) and using the unmodified value of τ_D for the rescaling of the MFPT in fig. 2(a).

This demonstrates that for a memory time τ_1 that is long compared to the diffusion time, that means for $\tau_1/\tau_D \gg 1$, the effect of the exponential memory contribution proportional to γ_1 on the MFPT disappears, as has been shown for the symmetric friction case $\gamma_1 = \gamma_2$ before [29]. For $\tau_2/\tau_D = 0.1$ and $\tau_2/\tau_D = 0.316$ the MFPT is almost constant over the entire range of τ_1/τ_D, which reflects the fact that for these values of τ_2/τ_D, in both limits $\tau_1/\tau_D \ll 1$ as well as $\tau_1/\tau_D \gg 1$, the MFPT is dominated by the overdamped contribution to the MFPT in eq. (10) and in fact is almost equal to the Markovian result, depicted by a horizontal dash-dotted line.

Next we investigate how the ratio between the two friction coefficients γ_2/γ_1 affects the MFPT. For this we show in fig. 2(b) the rescaled MFPT τ_{MFP}/τ_D as a function of γ_2/γ_1 for various values of τ_m/τ_D and fixed $\tau_1/\tau_D = 1$ and $\tau_2/\tau_D = 10$. There are some deviations between the simulation results and eq. (9), in particular for small γ_2/γ_1, but overall the heuristic formula constitutes a good approximation of our simulation results. We notice that in the left and the right parts of the figure, *i.e.*, for $\gamma_2 \ll \gamma_1$ and $\gamma_2 \gg \gamma_1$, respectively, τ_{MFP} becomes constant. The black horizontal lines denote the predictions of the heuristic formula in the single-exponential case for $\gamma_1 = 0$ on the right and for $\gamma_2 = 0$ on the left. As expected, as the amplitude of one of the two exponential contributions to the memory kernel becomes substantially smaller than the amplitude of the other contribution, its effect on the MFPT disappears.

In fig. 2(c) the ratio between the memory times τ_2 and τ_1 is larger and corresponds to 100. Similarly to fig. 2(b), in the left and right parts of the plot the MFPTs saturate at constant values, but the crossover regime within which the MFPT depends on the friction coefficient ratio γ_2/γ_1 is larger. While in fig. 2(b), where $\tau_2/\tau_1 = 10$, the crossover regime spans two orders of magnitude in γ_2/γ_1, the crossover regime in fig. 2(c), where $\tau_2/\tau_1 = 100$, extends over four orders of magnitude in γ_2/γ_1. This suggests already that the scaling variable that describes the relative importance of exponential memory contributions is proportional to γ_i/τ_i^2, which further below we will derive from the heuristic formula eq. (9). To demonstrate the memory effects on the MFPT, also in fig. 2(b) and (c) we represent the Markovian limit by horizontal dash-dotted lines.

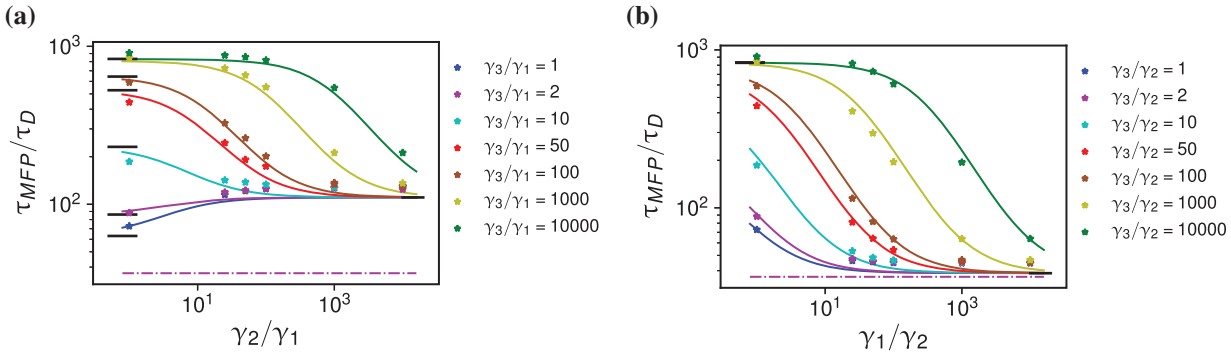

Fig. 3: Mean first-passage time for tri-exponential memory for fixed $\tau_m/\tau_D = 1$, $\tau_1/\tau_D = 0.316$, $\tau_2/\tau_D = 1$, $\tau_3/\tau_D = 3.16$ and $U_0/k_BT = 3$. In (a) we plot the simulation results for the rescaled MFPT τ_{MFP}/τ_D as a function of γ_2/γ_1, differently colored stars represent simulation results for various values of γ_3/γ_1. In (b), τ_{MFP}/τ_D is shown as a function of γ_1/γ_2 for various values of γ_3/γ_2. In both plots colored lines represent the heuristic formula (9) and the horizontal black lines to the right represent eq. (9) for single-exponential memory, in (a) for $\gamma_1 = \gamma_3 = 0$ and in (b) for $\gamma_2 = \gamma_3 = 0$, while the horizontal black lines to the left represent eq. (9) for bi-exponential memory. The horizontal black lines in (b) to the left are for $\gamma_3/\gamma_2 = 1000$ and 10000 and lie on top of each other. The dash-dotted horizontal lines denote the Markovian limit for $\tau_1 = \tau_2 = \tau_3 = 0$.

We now consider triple-exponential memory kernels, which are characterized by three friction coefficients γ_1, γ_2, γ_3 and three rescaled memory times τ_1/τ_D, τ_2/τ_D, τ_3/τ_D and τ_m/τ_D. In fig. 3 we compare simulation data with the heuristic formula (9). In the two plots, the MFPT is shown as a function of γ_2/γ_1 and γ_1/γ_2 for various fixed values of γ_3/γ_1 and γ_3/γ_2, respectively, and for fixed values of $\tau_1/\tau_D = 0.316$, $\tau_2/\tau_D = 1$, $\tau_3/\tau_D = 3.16$. In both plots we observe good agreement between the heuristic formula, shown by solid lines, and the simulation data, shown by stars, demonstrating the validity of the heuristic formula also for tri-exponential memory kernels. This suggests that the heuristic formula (9) holds also for any multi-exponential memory.

We also observe in fig. 3 in both plots, that τ_{MFP}/τ_D reaches the single-exponential limit, marked by a horizontal black line to the right, if the amplitude of one memory kernel becomes very large, *i.e.*, for $\gamma_2/\gamma_1 \to \infty$ in fig. 3(a) and $\gamma_1/\gamma_2 \to \infty$ in fig. 3(b). If the amplitude of one exponential memory contribution becomes very small, *i.e.*, for $\gamma_2/\gamma_1 \to 0$ in fig. 3(a) and $\gamma_1/\gamma_2 \to 0$ in fig. 3(b), the bi-exponential memory kernel limit is asymptotically approached, which is marked by horizontal black lines to the left.

In fig. 4 we show simulation data for the rescaled MFPT τ_{MFP}/τ_D for bi-exponential memory as a function of the rescaled barrier height U_0/k_BT and compare with the heuristic formula (9). We observe good agreement for barrier heights larger than $U_0/k_BT \geq 2$ for all three friction coefficient ratios $\gamma_2/\gamma_1 = 0.1, 2, 10$. This means that the asymptotic exponential scaling of MFPT, dominated by the exponential $\tau_{MFP} \sim e^{U_0/k_BT}$ and which corresponds to the classical Arrhenius law, is already realized for quite small barrier heights.

We thus have established that the heuristic formula for the MFPT, eq. (9), is a good approximation for multi-exponential memory kernels with general friction

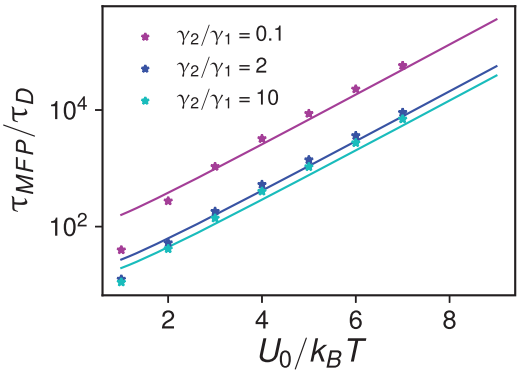

Fig. 4: Bi-exponential memory. Results for the rescaled MFPT τ_{MFP}/τ_D as a function of the rescaled barrier height U_0/k_BT for $\tau_m/\tau_D = 1$, $\tau_1/\tau_D = 10$ and $\tau_2/\tau_D = 1$ and different values $\gamma_2/\gamma_1 = 0.1, 2, 10$. The stars depict the simulation data and the lines depict the heuristic formula (9).

coefficients and memory times if the barrier height is larger than a few k_BT. Based on this validation, we will use that formula to investigate the global scaling behavior of τ_{MFP}. We first derive the proper scaling variables to be used in a global analysis of the MFPT. If we assume that for all memory times $\tau_i/\tau_D \gg 1$ holds, eq. (9) simplifies to

$$\frac{\tau_{MFP}}{\tau_D} \propto 4e^{\beta U_0}\left[\sum_i \left(\frac{\tau_D^2}{\tau_i^2}\frac{\gamma_i}{\gamma}\right)\right]^{-1}. \qquad (12)$$

This demonstrates that the MFPT in this limit depends on the scaling variables $[(\tau_D/\tau_i)^2\gamma_i/\gamma]^{-1}$ and that it is dominated by the exponential memory contribution for which $(\tau_D/\tau_i)^2\gamma_i/\gamma$ is largest. The scaling variables look at first sight counter-intuitive, since one would expect the effect of an exponential memory contribution to be proportional to its memory time. However, barrier crossing in the energy-diffusion limit is dominated by

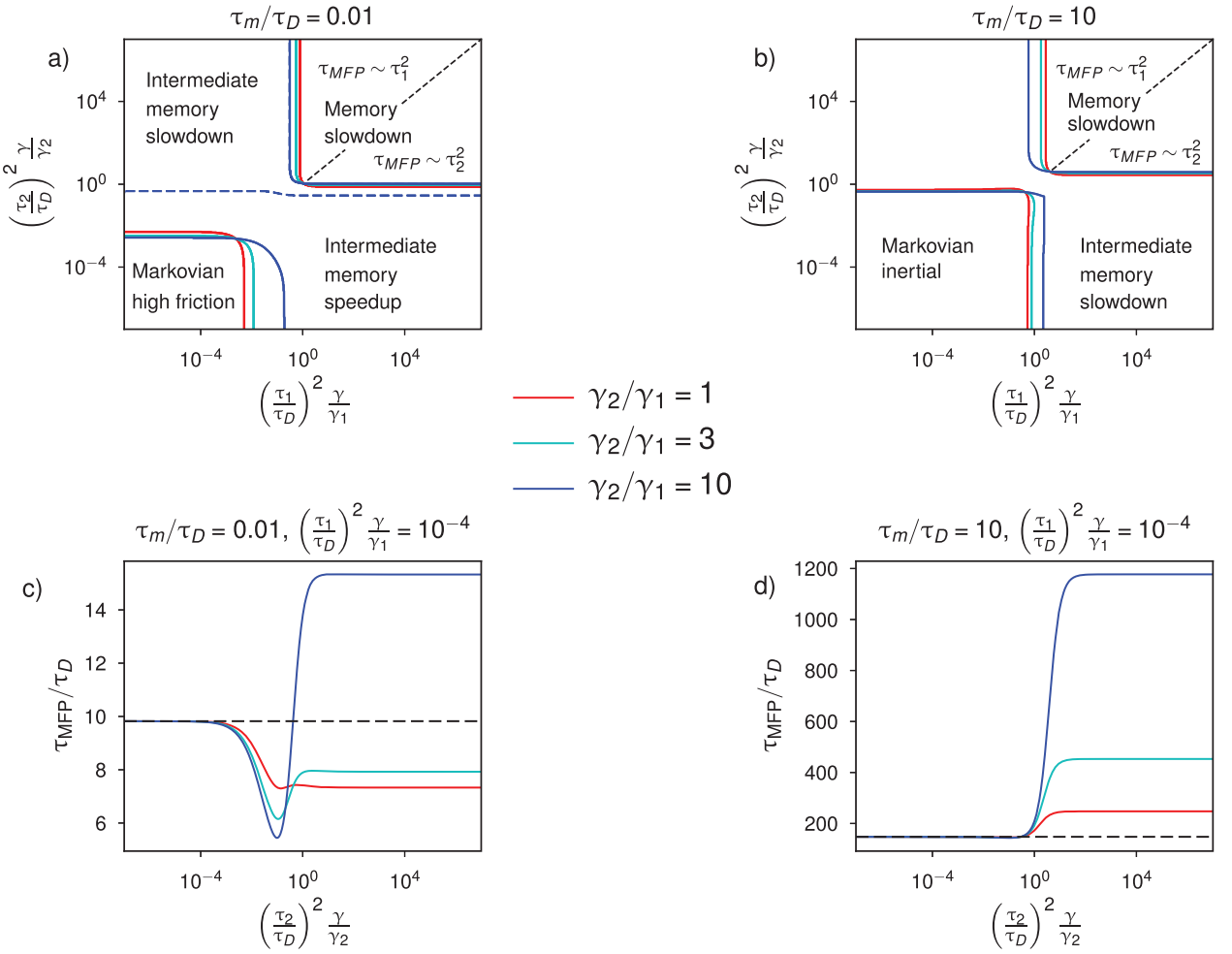

Fig. 5: (a) and (b): scaling diagrams for the MFPT in the presence of bi-exponential memory, based on the heuristic formula (9) as a function of the scaling variables $(\tau_1/\tau_D)^2\gamma/\gamma_1$ and $(\tau_2/\tau_D)^2\gamma/\gamma_2$ for $U_0/k_BT = 3$ and three ratios of the friction coefficients $\gamma_2/\gamma_1 = 1, 3, 10$. The transition from the Markovian regime to the intermediate memory speed-up regime is defined by the location where τ_{MFP} is smaller by 5% than the value in the Markovian limit ($\tau_1 = \tau_2 = 0$). The transition from the Markovian regime to the intermediate memory slowdown regime is defined by the location where τ_{MFP} is larger by 5% than the value in the Markovian limit. The asymptotic memory slowdown regime is defined where τ_{MFP} is ten times the value in the Markovian limit. Results are shown for the high-friction case $\tau_m/\tau_D = 0.01$ in (a) and for the low-friction regime $\tau_m/\tau_D = 10$ in (b). The dashed blue line in (a) represents the transition between the intermediate memory speed-up regime and the intermediate memory slowdown regime, the intermediate memory slowdown regime is for $\tau_m/\tau_D = 0.01$ only present for $\gamma_2/\gamma_1 = 10$. The dashed black diagonal lines in (a) and (b) in the asymptotic memory slowdown regime indicate the crossover from the τ_1-dominated barrier crossing for $\tau_1^2/\gamma_1 \ll \tau_2^2/\gamma_2$, to the τ_2-dominated barrier crossing for $\tau_2^2/\gamma_2 \ll \tau_1^2/\gamma_1$. One sees that the Markovian regime is entered when both $(\tau_1/\tau_D)^2\gamma/\gamma_1$ and $(\tau_2/\tau_D)^2\gamma/\gamma_2$ become small. Conversely, the asymptotic memory slowdown regime is entered when both $(\tau_1/\tau_D)^2\gamma/\gamma_1$ and $(\tau_2/\tau_D)^2\gamma/\gamma_2$ become large. The two asymptotic regimes are separated by intermediate slowdown or speed-up regimes. The small deviation between the scaling boundaries for the three different ratios of the friction coefficients $\gamma_2/\gamma_1 = 1, 3, 10$ demonstrates that the scaling diagram in terms of the scaling variables $(\tau_1/\tau_D)^2\gamma/\gamma_1$ and $(\tau_2/\tau_D)^2\gamma/\gamma_2$ describes the global behavior very well and leads to a diagram that is almost independent of γ_2/γ_1. In (c) and (d) the rescaled MFPT τ_{MFP}/τ_D is plotted according to eq. (9) as a function of $(\tau_2/\tau_D)^2\gamma/\gamma_2$ for fixed $(\tau_1/\tau_D)^2\gamma/\gamma_1 = 10^{-4}$ for different fixed ratios γ_2/γ_1 for $\tau_m/\tau_D = 0.01$ in (c) and for $\tau_m/\tau_D = 10$ in (d). The dashed horizontal lines denote the Markovian limit, obtained from eq. (9) by setting $\tau_1 = \tau_2 = 0$.

slow energy exchange between particle and heat bath. In this limit, the barrier crossing rate for multi-exponential memory is the sum of the individual barrier-crossing rates of each single-exponential memory contribution and is thus dominated by the memory contribution with the shortest memory time, which most quickly can exchange energy [41].

We therefore construct scaling diagrams for the behavior of τ_{MFP} for bi-exponential memory as a function of the inverse scaling variables $(\tau_1/\tau_D)^2\gamma/\gamma_1$ and $(\tau_2/\tau_D)^2\gamma/\gamma_2$. In fig. 5(a) we present the scaling diagram of the MFPT for high friction, $\tau_m/\tau_D = 0.01$, and in fig. 5(b) for low friction, $\tau_m/\tau_D = 10$, for various values of γ_2/γ_1, based on a numerical analysis of the heuristic formula

for the MFPT equation (9). For short rescaled memory times $(\tau_1/\tau_D)^2\gamma/\gamma_1 \to 0$ and $(\tau_2/\tau_D)^2\gamma/\gamma_2 \to 0$ the Markovian regime is obtained, where memory effects are absent. Depending on whether the friction is large or small, this Markovian regime corresponds to the Markovian high-friction regime or the Markovian inertial regime. We define the transition to the asymptotic memory slowdown regime, which is observed when $(\tau_1/\tau_D)^2\gamma/\gamma_1$ and $(\tau_2/\tau_D)^2\gamma/\gamma_2$ are both large, by the location where τ_{MFP} is ten times the value in the Markovian limit, defined by $\tau_1 = \tau_2 = 0$. The dashed black diagonal lines in the asymptotic memory slowdown regime indicate the crossover from the asymptotic scaling behavior $\tau_{MFP} \sim \tau_1^2$ for $\tau_1^2/\gamma_1 \ll \tau_2^2/\gamma_2$, to the asymptotic scaling behavior $\tau_{MFP} \sim \tau_2^2$ for $\tau_2^2/\gamma_2 \ll \tau_1^2/\gamma_1$. Between the Markovian regime and the asymptotic memory slowdown regime two different intermediate regimes exist. We define the transition between the Markovian regime and the intermediate memory speed-up regime by the location where τ_{MFP} is smaller than the Markovian limiting result by 5%. Analogously, we define the transition between the Markovian regime and the intermediate memory slowdown regime by the location where τ_{MFP} is larger than the Markovian limiting result by 5%. The intermediate memory speed-up regime in the high-friction limit, which was first observed for single-exponential memory [24], can be intuitively understood by the fact that memory friction pushes the particle towards the barrier after an unsuccessful barrier-crossing attempt and therefore accelerates the barrier crossing. In fig. 5(a) we observe both the intermediate memory speed-up regime and the intermediate memory slowdown regime for $\gamma_2/\gamma_1 = 10$, the transition between these two intermediate regimes is denoted by a blue broken line. For the other values of γ_2/γ_1 the intermediate memory slowdown regime is absent, which is why there is only a blue broken line visible. We observe that the intermediate regimes slightly shrink in size as the ratio γ_2/γ_1 increases, particularly in the direction of $(\tau_1/\tau_D)^2\gamma/\gamma_1$. Nevertheless, we conclude that the global behavior of the MFPT can be very efficiently described in terms of the scaling variables $(\tau_1/\tau_D)^2\gamma/\gamma_1$ and $(\tau_2/\tau_D)^2\gamma/\gamma_2$.

In fig. 5(c) and (d) we show the rescaled MFPT as a function of $(\tau_2/\tau_D)^2\gamma/\gamma_2$ for fixed $(\tau_1/\tau_D)^2\gamma/\gamma_1 = 10^{-4}$ in the high and low-friction regimes, this corresponds to vertical paths in the scaling diagrams. In fig. 5(c) we see that for small values of $(\tau_2/\tau_D)^2\gamma/\gamma_2$, τ_{MFP}/τ_D has the same value as in the Markovian regime, indicated by a dashed horizontal line. Increasing the value of $(\tau_2/\tau_D)^2\gamma/\gamma_2$ the barrier crossing accelerates as one enters the intermediate memory speed-up regime and τ_{MFP}/τ_D decreases. For $\gamma_2/\gamma_1 = 10$, τ_{MFP}/τ_D increases as $(\tau_2/\tau_D)^2\gamma/\gamma_2$ grows further as one enters the intermediate memory slowdown regime, but the asymptotic memory slowdown regime is not entered. For $\gamma_2/\gamma_1 = 3$, τ_{MFP}/τ_D slightly increases but does not become larger than the Markovian limit, therefore one stays in the intermediate memory speed-up regime. In fig. 5(d) we see that the MFPT τ_{MFP}/τ_D increases monotonically as $(\tau_2/\tau_D)^2\gamma/\gamma_2$, increases, indicating the intermediate memory slowdown regime.

Conclusion. – We studied numerically the barrier crossing of a massive particle in a one-dimensional double-well potential based on the generalized Langevin equation in the presence of bi- and tri-exponential memory kernels. We particularly studied the case where the different exponential contributions have different amplitudes and validated the heuristic crossover formula (9) that was previously introduced based on simulations for bi-exponential memory with equal friction amplitudes $\gamma_1 = \gamma_2$. Based on that heuristic formula, we show that the relative effect of different exponential memory contributions on the MFPT is described by the scaling variable $(\tau_D/\tau_i)^2\gamma_i/\gamma$, which is given by the rescaled ratio of the individual friction coefficient γ_i and the squared memory time τ_i^2. A global diagram for the scaling behavior of the MFPT is constructed in terms of these scaling variables for bi-exponential memory. In that scaling diagram the Markovian regime for small memory times is separated from the asymptotic memory slowdown regime by intermediate regimes, where the MFPT is slightly larger or smaller than in the Markovian regimes, depending on the parameters.

The scaling diagrams derived here look similar to the scaling digrams derived previously for the restricted case of bi-exponential memory with equal friction amplitudes $\gamma_1 = \gamma_2$ [29], but are in fact much more general since by use of the scaling variables $(\tau_D/\tau_1)^2\gamma_1/\gamma$ and $(\tau_D/\tau_2)^2\gamma_2/\gamma$ they apply to the general case where the friction amplitudes γ_1 and γ_2 are unequal. As a main result, we find that in the non-Markovian limit, the barrier-crossing time becomes dominated by the memory contributions that are characterized by the largest scaling variables $(\tau_D/\tau_i)^2\gamma_i/\gamma$.

* * *

This research has been funded by Deutsche Forschungsgemeinschaft (DFG) through Grant No. CRC 1114 "Scaling Cascades in Complex Systems", Project Number 235221301, Project B3 "Multilevel coarse graining of multiscale problems" and by European Research Council under the EU's Horizon 2020 Program, Grant No. 740269.

Appendix

The generalized Langevin equation can be rewritten as the coupled set of dimensionless Markovian equations

$$\dot{\tilde{x}}(\tilde{t}\,) = \tilde{z}(\tilde{t}\,), \tag{A.1}$$

$$\frac{\tau_m}{\tau_D}\dot{\tilde{z}}(\tilde{t}\,) = \sum_{i=1}^{N}\frac{\tau_D}{\tau_i}\frac{\gamma_i}{\gamma}[\tilde{y}_j(\tilde{t}\,) - \tilde{x}(\tilde{t}\,)] + \tilde{F}(\tilde{x}(\tilde{t}\,)), \tag{A.2}$$

$$\dot{\tilde{y}}_i(\tilde{t}\,) = -\frac{\tau_D}{\tau_i}[\tilde{y}_i(\tilde{t}\,) - \tilde{x}(\tilde{t}\,)] + \sqrt{\frac{\gamma}{\gamma_i}}\tilde{\xi}_i(\tilde{t}\,), \quad 1 \le i \le N, \tag{A.3}$$

where $\tilde{t} = t/\tau_D$, $\tilde{x}(\tilde{t}) = x(\tau_D\tilde{t})/L$, $\tilde{z}$ and the $\tilde{y}_i$ are auxiliary variables, $\tilde{F}(\tilde{x}) = (k_BT)^{-1}LU'(L\tilde{x})$, dots on top of

functions denote derivatives with respect to $\tilde{t}$, and the correlators of the dimensionless random forces $\tilde{\xi}_i(\tilde{t}) := (k_BT)^{-1}L\, f_{R_i}(\tau_D\tilde{t})$ are given by

$$\langle\tilde{\xi}_i(\tilde{t})\tilde{\xi}_j(\tilde{t}')\rangle = 2\delta(\tilde{t}-\tilde{t}')\delta_{ij}. \tag{A.4}$$

Solving the inhomogeneous harmonic-oscillator equation (A.3) for the auxiliary variable $\tilde{y}_i$, substituting the result into eq. (A.2), it is seen that eqs. (A.1)–(A.4) are equivalent to the GLE equations (1), (2) [29]. In the simulations we used eqs. (A.1)–(A.4) with the 4th-order Runge-Kutta method. The time step was fixed at $\Delta\tilde{t} = \Delta t/\tau_D = 0.01 \cdot \min\{\tau_m/\tau_D, \tau_1/\tau_D, \tau_2/\tau_D, 1\}$.

REFERENCES

[1] Berezhkovskii A. and Szabo A., *J. Chem. Phys.*, **122** (2005) 014503.
[2] Bryngelson J. D., Onuchic J. N., Socci N. D. and Wolynes P. G., *Proteins: Struct. Funct. Genet.*, **21** (1995) 167.
[3] Bryngelson J. D. and Wolynes P. G., *J. Phys. Chem*, **93** (1989) 6902.
[4] Dudko O., Hummer G. and Szabo A., *Phys. Rev. Lett.*, **96** (2006) 108101.
[5] Socci N. D., Onuchic J. N. and Wolynes P. G., *J. Chem. Phys.*, **104** (1996) 5860.
[6] Kramers H. A., *Physica*, **7** (1940) 284.
[7] Chandler D., *J. Stat. Phys.*, **42** (1986) 49.
[8] Berne B. J., Borkovec M. and Straub J. E., *J. Phys. Chem.*, **92** (1988) 3711.
[9] Hänggi P., Talkner P. and Borkovec M., *Rev. Mod. Phys.*, **62** (1990) 251.
[10] Best R. and Hummer G., *Phys. Rev. Lett.*, **96** (2006) 228104.
[11] de Sancho D., Sirur A. and Best R. B., *Nat. Commun.*, **5** (2014) 4307.
[12] Lange O. F. and Grubmüller H., *J. Chem. Phys.*, **124** (2006) 214903.
[13] Rosenberg R. O., Berne B. J. and Chandler D., *Chem. Phys. Lett.*, **75** (1980) 162.
[14] Sancho J. M., Romero A. H. and Lindenberg K., *J. Chem. Phys.*, **109** (1998) 9888.
[15] Zuckerman D. M. and Woolf T. B., *J. Chem. Phys.*, **116** (2002) 2586.
[16] Li Z., Bian X., Li X. and Karniadakis G. E., *J. Chem. Phys.*, **143** (2015) 243128.
[17] Rey R. and Guardia E., *J. Phys. Chem.*, **96** (1992) 4712.
[18] Mullen R. G., Shea J.-E. and Peters B., *J. Chem. Theor. Comput.*, **10** (2014) 659.
[19] Plotkin S. S. and Wolynes P. G., *Phys. Rev. Lett.*, **80** (1998) 5015.
[20] Das A. and Makarov D. E., *J. Phys. Chem. B*, **122** (2018) 9049.
[21] Mitterwallner B. G., Schreiber C., Daldrop J. O., Rädler J. O. and Netz R. R., *Phys. Rev. E*, **101** (2020) 032408.
[22] Kowalik B., Daldrop J. O., Kappler J., Schulz J. C. F., Schlaich A. and Netz R. R., *Phys. Rev. E*, **100** (2019) 012126.
[23] Jung G., Hanke M. and Schmid F., *Soft Matter*, **14** (2018) 9368.
[24] Kappler J., Daldrop J. O., Brünig F. N., Boehle M. D. and Netz R. R., *J. Chem. Phys.*, **148** (2018) 014903.
[25] Lesnicki D., Vuilleumier R., Carof A. and Rotenberg B., *Phys. Rev. Lett.*, **116** (2016) 147804.
[26] Daldrop J. O., Kowalik B. G. and Netz R. R., *Phys. Rev. X*, **7** (2017) 041065.
[27] Tolokh I. S., White G. W. N., Goldman S. and Gray C. G., *Mol. Phys.*, **100** (2002) 2351.
[28] Gottwald F., Karsten S., Ivanov S. D. and Kuühn O., *J. Chem. Phys.*, **142** (2015) 244110.
[29] Kappler J., Hinrichsen V. B. and Netz R. R., *Eur. Phys. J. E*, **42** (2019) 119.
[30] Zwanzig R., *Phys. Rev.*, **124** (1961) 983.
[31] Schmidt J., Meistrenko A., van Hees H., Xu Z. and Greiner C., *Phys. Rev. E*, **91** (2015) 32125.
[32] Mori H., *Prog. Theor. Phys.*, **33** (1965) 423.
[33] Grote R. F. and Hynes J. T., *J. Chem. Phys.*, **73** (1980) 2715.
[34] Pollak E., Grabert H. and Hänggi P., *J. Chem. Phys.*, **91** (1989) 4073.
[35] Jung G., Hanke M. and Schmid F., *J. Chem. Theory Comput.*, **13** (2017) 2481.
[36] Meyer H., Pelagejcev P. and Schilling T., *EPL*, **128** (2019) 052140.
[37] Peters A. J., Nation B. D., D. N., Ludovice P. J. and Henderson C. L., *Macromol. Theory Simul.*, **27** (2018) 1700062.
[38] Straub J. E., Borkovec M. and Berne B. J., *J. Chem. Phys.*, **84** (1986) 1788.
[39] Bao J.-D., Li R.-W. and Wu W., *J. Comput. Phys.*, **197** (2004) 241.
[40] Tocino A. and Ardanuy R., *J. Comput. Appl. Math.*, **138** (2002) 219.
[41] Talkner P. and Braun H.-B., *J. Chem. Phys.*, **88** (1988) 7537.